Environmental Science: Atmospheres

ROYAL SOCIETY OF CHEMISTRY

PAPER

View Article Online
View Journal | View Issue

Cite this: *Environ. Sci.: Atmos.*, 2025, **5**, 714

Two approaches to mass closure analysis for carbon-rich aerosol in Metro Manila, Philippines†

Grace Betito,*[abc] Grethyl Catipay-Jamero,[abd] Honey Alas,[e] Wolfram Birmili,[ef] Maria Obiminda Cambaliza,[ab] Mylene Cayetano,[g] David Cohen,[h] Melliza Cruz,[b] Maria Cecilia Galvez,[i] Arvin Jagonoy,[j] Simonas Kecorius,[kl] Genevieve Rose Lorenzo,[b] Leizel Madueño,[e] Thomas Müller,[e] Preciosa Corazon Pabroa,[j] James Bernard Simpas,[ab] Armin Sorooshian,[cm] Everlyn Gayle Tamayo,[g] Edgar Vallar,[i] Kay Weinhold[e] and Alfred Wiedensohler[e]

In this paper, we investigate physico-chemical properties of particulate matter (PM) at an urban mixed site (UB) and two roadside (RS) sites during the 2015 Metro Manila Aerosol Characterization Experiment (MACE). Aerosol particle number size distributions (0.01–10 μm diameter) were measured using a combination of a mobility particle size spectrometer and aerodynamic particle size spectrometers. $PM_{2.5}$ filter samples were analyzed for total mass, organic carbon (OC), elemental carbon (EC), water-soluble inorganic ions, and elemental species. Mass closure between the gravimetric mass, chemical composition, and mass concentration derived from the number size distribution was performed. We found that the bulk $PM_{2.5}$ mass was dominated by carbonaceous materials, followed by secondary inorganic aerosols and crustal matter at all sites. The average OC/EC ratios at the RS sites (0.16–1.15) suggest that a major fraction of the aerosol mass at these sites derives from traffic sources, while the OC/EC ratio at the UB site (2.92) is indicative of a more aged aerosol, consistent with greater contribution from secondary organic carbon (SOC) formation. The ultrafine particles (UFPs, diameter < 100 nm) dominated (89–95%) the total particle number concentration at the three sites, highlighting the importance of such measurements in this region. However, UFPs have low mass contribution to $PM_{2.5}$ (7–18%), while particles in the accumulation mode (diameter 100–1000 nm) accounted for most of the number-derived $PM_{2.5}$ mass concentration (61–67%). On average, strong agreement between the chemically-derived mass and the gravimetric mass was found (slope = 1.02; r^2 = 0.94). The number-derived mass concentration correlated well with the gravimetric $PM_{2.5}$ mass (slope = 1.06; r^2 = 0.81). These results highlight the need for more comprehensive PM characterization, particularly focusing on size-resolved chemical composition and particle number size distributions. The mass closure approach presented in this work provides a framework for a conversion between number size distributions and $PM_{2.5}$ mass concentration in real time in an environment with similar characteristics.

Received 23rd February 2025
Accepted 18th May 2025

DOI: 10.1039/d5ea00028a

rsc.li/esatmospheres

[a]*Department of Physics, Ateneo de Manila University, Katipunan Ave., Quezon City, Philippines*
[b]*Manila Observatory, Ateneo de Manila Campus, Quezon City, Philippines*
[c]*Department of Hydrology and Atmospheric Sciences, University of Arizona, Tucson, AZ, USA. E-mail: gbetito@arizona.edu*
[d]*Caraga State University-Cabadbaran Campus, Cabadbaran City, Agusan del Norte, Philippines*
[e]*Leibniz Institute for Tropospheric Research, Leipzig, Germany*
[f]*German Environment Agency (Umweltbundesamt), Berlin, Germany*
[g]*Institute of Environmental Science and Meteorology, University of the Philippines Diliman, Philippines*
[h]*Australian Nuclear Science and Technology Organization, Menai, Australia*
[i]*Environment and Remote Sensing Research (EARTH) Laboratory, Department of Physics, De La Salle University, Manila, Philippines*
[j]*Philippine Nuclear Research Institute – Department of Science and Technology, Quezon City, Philippines*
[k]*Institute of Epidemiology, Helmholtz Zentrum München – German Research Center for Environmental Health, Neuherberg, Germany*
[l]*Environmental Science Center, University of Augsburg, Augsburg, Germany*
[m]*Department of Chemical and Environmental Engineering, University of Arizona, Tucson, AZ, USA*

† Electronic supplementary information (ESI) available. See DOI: https://doi.org/10.1039/d5ea00028a

Environmental significance

Metro Manila, the capital region of the Philippines, is impacted by a diverse range of pollution sources, with road-traffic related emissions of black carbon significantly contributing to PM mass. While previous studies in the region have primarily focused on gravimetric and chemical analyses, recent studies suggest that particle number concentration (especially those of ultrafine particles) is more strongly linked to health effects. Here, we quantify PM mass, PM chemical composition, and particle number concentration to provide a more complete understanding of atmospheric composition in this megacity. Results reveal the importance of black carbon, organic matter, and ultrafine particles at the sampling sites. Mass closure was achieved between gravimetric, chemical composition, and number-derived mass concentrations. This study raises awareness of poor air quality in Metro Manila and motivates further research with longer sample collection periods, covering different seasons and expanding analysis beyond conventional PM metrics.

1 Introduction

Ambient particulate matter (PM) has significant impacts on human health,[1] visibility reduction,[2] ecosystem degradation,[3] and global climate.[4] Exposure to ambient PM can lead to deleterious health problems such as cardiovascular and respiratory diseases, incidents of lung cancer, and premature deaths.[5,6] The magnitude of the effect of PM on health depends on its chemical composition (toxicity) and deposition efficiency, which is mainly governed by particle size, hygroscopicity, shape, and density.[7]

In terms of PM mass concentration, currently only PM_{10} and $PM_{2.5}$ (aerodynamic particle diameter less than 10 μm and 2.5 μm, respectively) mass are regulated.[8] Traditional online, and filter-based PM sampling methods for mass concentrations are more common than size spectrometers. However, size spectrometers provide the key advantage of directly measuring particle number concentrations, which are more relevant to health impacts. To be able to relate to current air quality standards, particle number size distribution measurements, which provide comprehensive information about particle properties, must be converted to mass concentration. This conversion requires knowledge of particle density and shape to determine the relationship between mobility and aerodynamic diameters,[9] and to convert particle number size distributions to particle mass size distributions.[9–11]

Typically, particle density is determined indirectly by knowing the dominant chemical composition of PM of a certain size range.[12] However, particle density is affected by both physical and chemical characteristics, as well as generation processes of aerosol particles.[13] For example, particles from natural sources (*e.g.*, sea salt and mineral dust) have densities relatively higher than 1.0 g cm^{-3} due to a more compact structure, while freshly emitted combustion particles are more loosely aggregated and usually have densities lower than 1.0 g cm^{-3}.[7,13] Combustion is a major source of fine and ultrafine particles (UFPs, diameter < 100 nm),[12,14–16] with diesel-powered engines emitting large quantities of agglomerate soot particles.[17] Although UFPs contribute less to total PM mass compared to the fewer but larger particles, they represent the largest portion of the total particle number concentration.[18,19] Studies suggest that particle number concentration, rather than mass concentration, may be more strongly linked to health effects.[20,21] However, some studies in other Southeast Asian cities reported high mass concentration of UFPs[16,22,23] indicating the growing contribution of these tiny particles to total PM mass loading. Thus, it is important to not only quantify PM mass, but also particle number concentration, chemical composition, and the interrelationships among these parameters to better understand PM impacts.

Metro Manila, the capital region of the Philippines, is impacted by a complex source of particulate pollution, including traffic, aged aerosol, biomass burning, industrial, cooking activities, and waste processing.[24–28] A special feature of PM in Metro Manila is the high concentration and lack of seasonality of black carbon (BC).[29–31] At an urban mixed site, BC is approximately 30% of $PM_{2.5}$ mass[24,28] in contrast to 45% at a roadside site,[32] and 55–75% for equivalent BC (eBC,[33] a proxy for soot measured optically) at a street site.[26] At a roadside site, hourly concentrations of eBC as high as 138 μg m^{-3} were observed.[34] Speciated particle mass size distribution measurements by Cruz *et al.*[25] revealed that BC mainly resides in the submicrometer range, peaking between 0.18–0.32 μm diameter, with its total mass accounting for 26.9% of the total PM mass. These studies have highlighted the considerable contribution of BC to the PM loading in the region compared to other polluted neighbouring countries.[29]

This study tackles the issue of mass concentration closure of ambient PM based on multiple measurements related to particle number size distributions and chemical composition. Mass closure analysis aims to provide a consistent picture of how ambient PM is structured physically and chemically,[35–37] which is highly relevant for a consistent understanding of its sources, transformation processes and subsequent atmospheric and health effects. On an experimental level, mass closure also indicates the compatibility and quality of all the PM measurements involved, and helps estimate parameters such as particle shape and density, which often cannot be measured directly. In this investigation, mass closure was performed in two ways: (i) between gravimetric $PM_{2.5}$ mass and the cumulative sum of identified chemical components including organic carbon (OC), elemental carbon (EC), secondary inorganic aerosols, crustal and trace elements; and (ii) between gravimetric $PM_{2.5}$ mass and the particle number-derived mass measured from different size spectrometers. The latter addresses the challenge of synthetizing data from a mobility particle size spectrometer (MPSS) and an aerodynamic particle size spectrometer (APSS) that provide different particle metric diameters (*e.g.*, mobility diameter and aerodynamic diameter). This work provides, for the first time, particle number-derived mass distributions and a closure between gravimetric and number-derived mass in the BC-dominated and highly populated Metro Manila area, where PM-related health effects are anticipated to be significant.

2 Experimental methods

2.1 Sampling site

Aerosol particle physico-chemical properties were measured at three sites in Metro Manila from April to June 2015 as part of the Metro Manila Aerosol Characterization Experiment (MACE) campaign (Fig. 1). This campaign was a collaboration between the Leibniz Institute for Tropospheric Research (TROPOS) and the "Researchers for Clean Air" (RESCueAir) consortium including Ateneo de Manila University (ADMU), De La Salle University (DLSU), Manila Observatory (MO), University of the Philippines-Diliman (UPD), and the Department of Science and Technology – Philippine Nuclear Research Institute (DOST-PNRI).

The Katipunan Avenue roadside site (14.635° N, 121.075° E) (referred to as "KAT RS") was situated within the ADMU campus and ~2 m from Katipunan Avenue, a four-lane (each direction) major road in Quezon City. The site is ~350 m north of a public utility jeepney (PUJ) vehicle terminal, which is situated along the intersection of Katipunan Avenue and several other main roads that carry heavy traffic, especially during rush hours. Alongside the main road are residential apartment buildings, condominiums, commercial establishments, and fast-food restaurants. Size spectrometers and filter-based PM sampling were performed from 3 April to 5 May 2015.

The MO urban mixed site (14.636° N, 121.078° E), referred to as "MO UB", was located within the ADMU campus and ~350 m east of the KAT RS site. This station is surrounded by trees. Size spectrometers and filter-based PM sampling were conducted from 8 to 15 May 2015, coinciding with a period of no summer classes and thus less vehicular traffic in the immediate vicinity as compared to regular school session periods.

Another roadside site (14.566° N, 120.994° E) was situated along Taft Avenue, Manila (referred to as "TAFT RS") and is adjacent to the DLSU campus. The three-lane (each direction) road under the light-rail transit (LRT) railway is congested by PUJs, public utility vans (PUVs), buses, and taxis. This site resembles a street canyon because of its narrow road that is situated under the LRT railway, with towering condominiums and commercial establishments surrounding this area. The

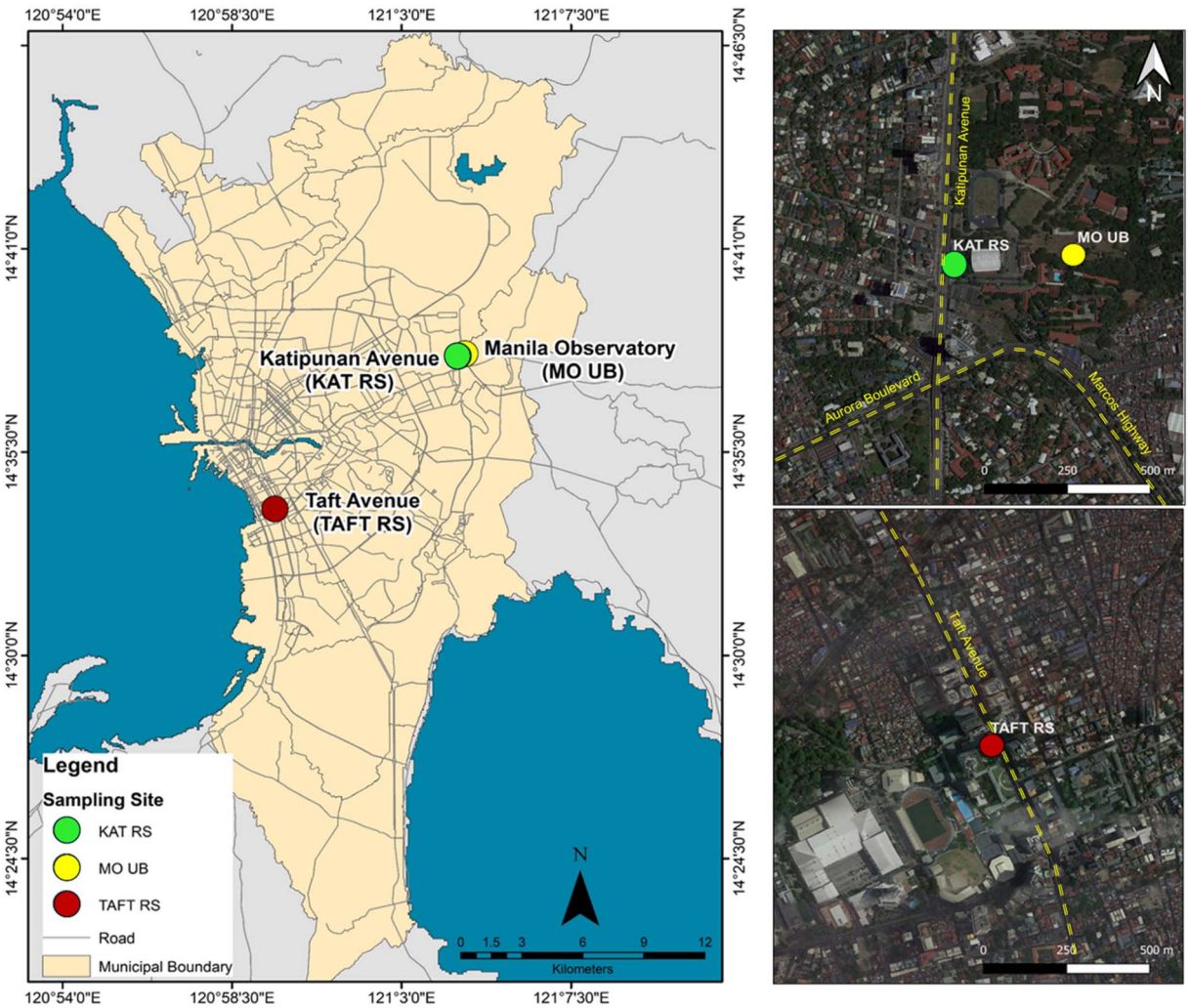

Fig. 1 Study area with locations marked for the three sampling sites during the 2015 MACE campaign. The right panel is the zoomed-in version of sampling sites. Right image source: Google Earth.

instruments were situated at ~0.5 m from the street curb. Size spectrometers and filter-based PM sampling were conducted from 18 May to 9 June 2015.

2.2 Meteorological conditions

Meteorological data (wind speed and direction) were collected using an automatic weather station (Davis Vantage Pro2 Plus, Davis Instruments Corp. Inc., California, USA) installed on top of the measurement container. At the KAT RS site, the prevailing wind is from the south-southwest (Fig. S1a†), making KAT RS a downwind site of major thoroughfares (Aurora Boulevard and Marcos Highway) (Fig. 1). Traffic congestion intensifies at the highway during rush hour periods, which typically are 07:00–09:00 and 16:00–18:00 local time.[38] At the MO UB site, winds are coming from the west and east (Fig. S1b†), where Katipunan Avenue and the Marikina residential area are situated, respectively. Farther east of the Marikina residential area are the Sierra Madre mountains, which are relatively remote. The prevailing wind at the TAFT RS roadside is coming from the south-southeast direction (Fig. S1c†) where residential areas and large shopping malls are located.

To identify possible impact of long-range transport of PM to the study region, analysis of backward air mass trajectories was conducted using the NOAA Hybrid Single Particle Lagrangian Integrated Trajectory (HYSPLIT) model.[39,40] Trajectories were calculated for an end time of midnight local time and height of 500 m above ground level. Meteorological data were used from the Global Data Analysis System (GDAS1; 1° × 1° resolution). The five-day back trajectory analysis (Fig. S2†) revealed that during the measurement campaign (April–June), the prevailing air masses came from the open ocean suggesting minimal influence from long-range continental sources in neighboring countries.

2.3 Sample collection

Aerosol samples ($PM_{2.5}$) were collected using two low-flow air samplers (MiniVol, Airmetrics Inc., Oregon, USA) operating at 5 lpm. The samplers were installed on top of the measurement container approximately 7 m above the ground. Samples were collected using two types of filter substrates: Teflon (PTFE membrane, 2 μm pore size, 46.2 mm diameter, Whatman) and quartz (47 mm diameter Pallflex quartz-fiber, Whatman). The samplers were placed side by side and were programmed to run from midnight for a total of 24 hours. After sampling, Teflon filters were placed inside a temperature (20–23 °C) and relative humidity (30–40%) controlled room for at least 24 hours. Gravimetric analysis was performed using a Sartorius ME5-F microbalance with a sensitivity of ±1 μg (Sartorius, Göttingen, Germany).

Particle number size distribution (PNSD) across the mobility diameter range of 10–800 nm was measured using a TROPOS-type Mobility Particle Size Spectrometer (MPSS)[41] installed inside the measurement container. The MPSS included a Hauke-type Differential Mobility Analyzer (DMA) and TSI 3772 Condensation Particle Counter (CPC) with a flow rate of 1 lpm. Additionally, an aerodynamic particle size spectrometer (APSS, TSI 3321) was used to measure PNSD for the diameter range of 500 nm to 10 μm (aerodynamic diameter; limited by PM_{10} inlet at aerosol intake line). The MPSS and APSS sizing accuracies were calibrated using nebulized polystyrene latex spheres (PSL) of 203 nm and 2.0 μm (ThermoScientific™, Duke Standards™), respectively.

2.4 Chemical composition analysis

The concentrations of a suite of elements, including Al, Si, P, S, Cl, K, Ca, Ti, V, Cr, Mn, Fe, Ni, Cu, and Zn, were determined by Photon Induced X-ray Emission (PIXE). Concentrations obtained from this analysis are expressed in μg cm^{-2}. To convert it to μg m^{-3}, each value is multiplied by the filter area (11.81 cm^2) and divided by the volume of air sampled in 24 h (in m^3). After the elemental analysis, each Teflon filter was cut in half, with one half extracted in 14 ml of Milli-Q water (18.2 MΩ) through sonication for 1 h in a plastic 15 ml centrifuge vial. The aqueous extracts were analyzed for water-soluble ions (NH_4^+, K^+, Mg^{2+}, Ca^{2+}, Cl^-, NO_3^-, SO_4^{2-}) using an ion chromatography system (IC; Shimadzu). Pallflex quartz-fiber filters were prebaked at 900 °C for three hours prior to sampling.[42] OC and EC were then quantified with a Sunset Laboratory OC–EC Aerosol Analyzer following the edited Improve_A protocol (Table S1†).[42,43] The completion date of the chemical analyses was summarized in Table S2.†

2.5 Calculations and error discussion

2.5.1 Gravimetrically-derived mass concentration. The Teflon filters were weighed twice before and after sampling, with differences between duplicate weights being <10 μg. The calculated uncertainties in weighing were negligible, with the highest being ~0.8%. The PM mass in μg was derived from the average final substrate weight minus the initial substrate weight. The PM mass concentration in μg m^{-3} was calculated by dividing the total PM mass (μg) with the total volume of air sampled (m^3). Using the error propagation equation (eqn (S1)†),[44] the overall uncertainty of the gravimetric mass (due to the uncertainty in weighing, and uncertainty in sampling air volume) was approximately 5%. For our plots, we applied a 10% uncertainty to account for additional unquantified sources of uncertainty.

2.5.2 Chemically-derived mass concentration. The mass concentrations of water-soluble ions were calculated using a manually prepared calibration curve. For this study, five to six calibration standards per analyte were prepared using a reference standard. After creating the calibration curve, two to three check standards were run again to check the accuracy of the calibration. Recoveries were then calculated as the ratio between the mass of a specific measured species and the known amount of that species in that sample.[45] Recoveries were all above 95% with repeatability ranging from 8% to 20%. Another way to check the validity of the IC analysis is to perform the ion balance to determine potentially missing ionic species.[46] The molar ratio of cation equivalents (CE) and anion equivalents (AE) are used to infer the acidity of aerosol.[47] Assuming that aerosol particles are neutral, the ratio of the anion to cation

equivalence should be one. For this study, the ratios of AE/CE were higher than one (slope = 1.1; r^2 = 0.79), indicating cation deficiency. The AE/CE deficiency might be due to unmeasured H^+ ions.[48] For the elemental analysis using PIXE, error estimates were calculated using eqn (S2).†[49] The estimated uncertainty for OC and EC quantification ranged from 7% to 14%.

For the chemical mass balance, the chemical species were divided into eight classes as follows: (1) organic matter (OM), (2) EC, (3) sulfate, (4) nitrate, (5) ammonium, (6) sea salt, (7) crustal matter, and (8) trace elements. To convert OC to OM, correction factors were applied to estimate the average molecular weight per carbon weight for the organic aerosol.[50,51] For this study, a correction factor of 1.4 was used for the urban mixed site data, and 1.3 for the roadside data. These correction factor values were adapted from the study of Taiwo *et al.*[52] in the same type of environment. The OC to OM conversion is one of the major sources of uncertainty in chemical mass closure studies.[53] Sea-salt was estimated using the formula $1.8 \cdot Cl^-$ based on the relative abundance of Cl^- and Na^+ on a mass basis in seawater.[54] Crustal matter was calculated using the oxide forms of crustal species ($2.2 \cdot Al + 2.49 \cdot Si + 1.63 \cdot Ca + 2.42 \cdot Fe + 1.94 \cdot Ti$).[55] Trace elements were calculated by simply adding the concentrations of species Cr, Cu, Mn, Ni and Zn. Similarly, EC and secondary inorganic ions (sulfate, nitrate, and ammonium) were summed up without any extra modifications needed.[56,57] The unexplained mass was referred to as 'unknown'.

2.5.3 Number-derived particle mass size distribution. The determined PNSDs from the MPSS and APSS are based on different measurement principle. The MPSS classifies particles according to their mobility diameter (d_m) while the APSS does so according to aerodynamic diameter (d_a). To obtain PNSD from 10 nm to 10 μm, MPSS and APSS number size distributions were converted to volume-equivalent diameter (d_{ve}) using an enhanced inversion algorithm presented by Pfeifer *et al.*[58] In the merging process, an input density and dynamic shape factor are required. Selecting the particle density and shape factor is a crucial part in the inversion routine. These two parameters can be manipulated to achieve the best fit between the MPSS and APSS PNSDs. However, simultaneously changing both these parameters is difficult especially when processing thousands of PNSDs. For this study, we used a constant particle density value while varying the shape factors. The density value is usually based on the density of the major chemical components measured within the study area and is not directly obtained from a measuring instrument.[10,59] For this study, we assumed a particle density (1.8 g cm^{-3}) based on the dominant species in Metro Manila,[24,25,28] and using published densities for these species (OC – 1.2 g cm^{-3}, BC – 2.0 g cm^{-3}, $(NH_4)_2SO_4$ – 1.77 g cm^{-3}, NH_4NO_3 – 1.72 g cm^{-3}).[9] From the best fit between MPSS and APSS, a dynamic shape factor ranging from 1.1 to 2.3 was retrieved, falling within the range of shape factor values for soot reported in literature,[60,61] with an average of 1.6 (KAT RS), 1.4 (MO UB), and 2.0 (TAFT RS).

From the merged PNSDs ($dN/d\log D_p$), the particle mass size distribution (PMSD; $dM/d\log D_p$) was calculated using eqn (1) from Buonanno *et al.*:[62]

$$m_{mpss/apss,i} = \frac{\pi}{6} d_{ve}{}^3 \rho_p n_{mpss/apss,i} \quad (1)$$

where $m_{mpss/apss,i}$ is the mass concentration calculated from the combined MPSS + APSS number concentration ($n_{mpss/apss,i}$) in terms of volume equivalent diameter (d_{ve}), and particle density (ρ_p). Since the filter-based $PM_{2.5}$ is expressed in d_a, the equivalent of $PM_{2.5}$ to d_{ve} was determined using eqn (2) making use of the average shape factor identified at the three sites.

$$d_{ve} = d_a \sqrt{\frac{x \cdot \rho_0}{\rho_p}} \quad (2)$$

where x is the dynamic shape factor, ρ_0 is the reference density (1.0 g cm^{-3}), and ρ_p is the particle density (1.8 g cm^{-3}). The PMSDs were integrated for d_{ve} ranges of 0.1–2.5 μm for all sites to obtain the $PM_{2.5}$ mass concentration.

3 Results and discussion

3.1 $PM_{2.5}$ mass concentration and chemical composition

The average $PM_{2.5}$ mass concentration determined *via* the gravimetric method was 42.8 ± 9.3 μg m^{-3} at TAFT RS, 37.2 ± 11.9 μg m^{-3} at KAT RS, and 23.9 ± 7.2 μg m^{-3} at MO UB (Table 1). EC and OC contributed the most to $PM_{2.5}$ mass. Mass concentration of EC was highest at TAFT RS (20.8 ± 6.2 μg m^{-3}), followed by KAT RS (12.9 ± 3.3 μg m^{-3}), and the lowest at MO UB (4.4 ± 2.2 μg m^{-3}). For context, concentrations of EC at a few other sites in the Philippines are as follows: 6.63 μg m^{-3} (urban industrial site);[42] 2.29 μg m^{-3} (rural municipality area);[42] 0.67 μg m^{-3} (rural site);[63] and 9.0 μg m^{-3} (roadside site).[32] One explanation for the high EC concentrations at the roadside sites as compared to the urban mixed site is direct influence of traffic emissions[64,65] since measurements at both TAFT RS and KAT RS were carried out on and near the street. Moreover, the street canyon configuration of Taft Avenue restricts air circulation, leading to the accumulation of vehicular emissions in the area. Although trucks are prohibited along Taft Avenue, the road remains heavily used by private vehicles and PUJs.[34] Findings from Kecorius *et al.*[26] provide evidence that PUJ emissions contribute to the elevated eBC mass concentrations along Taft Avenue.

Mass concentrations of OC were 14.5 ± 3.8 μg m^{-3} (KAT RS), 9.0 ± 2.9 μg m^{-3} (MO UB), and 14.5 ± 3.8 μg m^{-3} (TAFT RS). Concentrations of OC are as follows for other studies in the country: 8.00 μg m^{-3} (urban industrial site);[42] 4.08 μg m^{-3} (rural municipality area);[42] and 1.15 μg m^{-3} (rural site).[63] OC is a complex mixture of different compounds produced *via* either direct emissions or produced by secondary processes (*i.e.*, gas-to-particle conversion).[66] Biomass burning and fossil fuel combustion are some of the major anthropogenic sources of OC.[64,67] There was a strong correlation between OC and K^+ at MO UB (r = 0.83) and TAFT RS (r = 0.65); these species were found to be associated with biomass burning (Table S3†).[68,69] Possible sources of these species at MO UB could be local biomass burning emission, especially coming from the east of the sampling area where the Sierra Madre mountains are located. At TAFT RS, aside from traffic, residential wood

Table 1 Summary (average ± standard deviation, in μg m^{-3}) of $PM_{2.5}$ mass, carbonaceous species, water-soluble ions, and elemental components analyzed at the three monitoring sites: Katipunan Avenue roadside site (KAT RS), Manila Observatory urban mixed site (MO UB), Taft Avenue roadside site (TAFT RS). Total number of collected filter samples (quartz and Teflon): KAT RS (16), MO UB (7), TAFT RS (9)

Species	KAT RS	MO UB	TAFT RS
$PM_{2.5}$	37.2 ± 11.9	23.9 ± 7.2	42.8 ± 9.3
OC	14.5 ± 3.8	9.0 ± 2.9	13.7 ± 3.5
EC	12.9 ± 3.3	4.4 ± 2.2	20.8 ± 6.2
Water-soluble ions			
NH_4^+	0.68 ± 0.66	0.72 ± 0.52	0.77 ± 0.42
K^+	0.33 ± 0.43	0.25 ± 0.12	0.15 ± 0.14
Mg^{2+}	0.05 ± 0.07	0.02 ± 0.01	0.03 ± 0.00
Cl^-	0.16 ± 0.17	0.08 ± 0.05	0.01 ± 0.00
NO_3^-	0.65 ± 0.30	0.63 ± 0.23	0.56 ± 0.32
SO_4^{2-}	2.52 ± 1.83	2.43 ± 1.28	2.87 ± 1.02
Elements			
Al	0.11 ± 0.06	0.11 ± 0.00	0.09 ± 0.02
Ca	0.14 ± 0.05	0.09 ± 0.04	0.15 ± 0.07
Cl	0.19 ± 0.15	0.11 ± 0.06	0.05 ± 0.01
Cr	0.02 ± 0.00	0.02 ± 0.00	0.00 ± 0.00
Cu	0.02 ± 0.01	0.01 ± 0.00	0.01 ± 0.00
Fe	0.24 ± 0.08	0.14 ± 0.08	0.21 ± 0.08
K	0.33 ± 0.26	0.22 ± 0.08	0.19 ± 0.08
Mn	0.01 ± 0.00	0.02 ± 0.01	0.02 ± 0.05
Ni	0.01 ± 0.00	0.02 ± 0.00	0.00 ± 0.00
S	0.87 ± 0.54	0.83 ± 0.46	0.97 ± 0.32
Si	0.43 ± 0.13	0.33 ± 0.04	0.34 ± 0.06
Ti	0.03 ± 0.01	0.00 ± 0.00	0.00 ± 0.00
Zn	0.10 ± 0.08	0.08 ± 0.06	0.09 ± 0.07

burning is also a likely source of OC, as well as meat cooking[70] since there are several grilling/barbecue restaurants operating near the sampling area.

The OC/EC ratio has been used as an indicator of the emission source and the transformation of carbonaceous aerosol. Values of OC/EC lower than 1 suggest that emissions of carbonaceous particles are dominated by traffic, greater than 2 implies secondary organic carbon (SOC) formation,[56] and between 4 and 6 signifies impacts from biomass burning or long-range transport from urban areas.[71] For this study, the mean OC/EC ratio was highest at MO UB (2.92), followed by KAT RS (1.15), and lowest at TAFT RS (0.68). An OC/EC ratio of 2.92 was also observed inside a university campus in Athens, Greece.[46] For TAFT RS, similar OC/EC ratios (<1) were observed in roadway tunnel studies in some regions of the world[72] such as Los Angeles, USA (0.76), southern Taiwan (0.4–0.6), and Marseille, France (0.53). The elevated OC/EC ratio at the MO UB indicates a clear prevalence of organic carbonaceous species over EC suggestive of possible SOC formation in that area. This can be attributed to the greater aging of the sampled air masses at MO UB site as compared to the other two sites. Aging helps generate secondary organic aerosols (SOA), a key player in OC formation.[73] On the other hand, since EC is directly emitted and not secondarily produced, aging does not produce it but instead dilutes its concentration.

To know the extent of the contribution of SOC to total OC, the equation proposed by Castro *et al.*[74] was used. The calculation uses the minimum OC/EC ratio of each site and assumes that $EC \times (OC/EC)_{min}$ represents primary OC. The SOC fraction is then calculated by:

$$SOC = OC - EC \times (OC/EC)_{min} \quad (3)$$

The highest SOC contribution was estimated at MO UB (52%) and is comparable to the value observed at a rural site (56.1%) in the Philippines (Angat, Bulacan).[42] This supports the assumption that the higher OC/EC ratio at MO UB was due to SOC formation. The SOC contributions to the total OC at the roadside sites were lower (KAT RS: 38%, TAFT RS: 28%) suggesting that there were more freshly emitted aerosols coming from traffic emissions.

Based on average ionic concentrations, SO_4^{2-} (2.43–2.87 μg m^{-3}) was the most abundant species for all sites, followed by NH_4^+ (0.68–0.77 μg m^{-3}), and NO_3^- (0.56–0.65 μg m^{-3}). Sulfate is formed secondarily from the oxidation of its precursor, SO_2, which is emitted *via* incomplete combustion of sulfur-containing fuels in vehicles and industries, and biomass burning.[64,75] Ammonium is derived from its precursor NH_3, which usually comes from agricultural activities and animal waste, but there is also some contribution arising from vehicle exhaust.[76,77] Nitrate is formed from the oxidation of NO_x with major local sources including gasoline- and diesel-powered engines, natural gas, and coal combustion.[78] Excellent correlation between SO_4^{2-} and NH_4^+ (r = 0.90–0.96) at the three sites suggests that NH_4^+ can be a neutralizing agent of SO_4^{2-} (Table S3†). For SO_4^{2-} to be completely neutralized, the NH_4^+/SO_4^{2-} molar ratio should be equal to 2 or higher.[46] For this study, the mean NH_4^+/SO_4^{2-} molar ratio (1.21–1.47) was lower than 2, which means that there was insufficient NH_4^+ to completely neutralize SO_4^{2-}. On the other hand, the correlation between NH_4^+ and NO_3^- (r = 0.35–0.58) is lower, suggesting that the formation of NH_4NO_3 was likely not favorable. At MO UB, nitrate is mainly in the coarse mode (1–3.2 μm) as it partitions to large aerosol types like salt and dust rather than making secondary salts like ammonium nitrate.[25]

Strong correlations between crustal species (Al, Si, Ca, and Fe) were also found at KAT RS (r = 0.68–0.85), MO UB (r = 0.94–0.97), and TAFT RS (r = 0.39–0.79) (Table S3†). An appreciable amount of a combination of trace elements (Cr, Cu, Ni, Mn, and Zn) was also measured at KAT RS (0.5 ± 0.3 μg m^{-3}), MO UB (0.3 ± 0.1 μg m^{-3}), and TAFT RS (0.3 ± 0.2 μg m^{-3}). It is known that Ca and Fe are associated with resuspended dust,[79,80] while Zn is commonly used in brake linings.[81,82] Another source of Ca is construction,[75] and we noted some construction activities near the roadside sites during the sampling period. The higher percentage of crustal matter at KAT RS and MO UB compared to TAFT RS is attributed partly to significant soil coverage in these sites, whereas, TAFT RS mostly has cemented/asphalted areas. The El Niño in 2015[83] heightened the dry conditions in these areas, so the soil is less covered with vegetation, and consequently had more efficient dust resuspension.

3.2 Particle number and number-derived mass size distribution

The combined number size distributions from the MPSS and APSS covered the total size range between 0.01–10 μm. In general, the shape of PNSD was similar at the three sites (Fig. 2a). Three modes can be observed: the nucleation mode (10–20 nm), accumulation mode (around 100 nm), and coarse mode (above 1000 nm). The average UFP number concentration was 9.6×10^4 cm^{-3} (KAT RS), 2.9×10^4 cm^{-3} (MO UB), and 7.7×10^4 cm^{-3} (TAFT RS) (Table 2). UFP concentration is higher at the roadside sites, reflecting the influence of traffic emissions. The average PNC at MO UB is at least two times lower than at RS sites because number concentrations of fine and UFPs decrease rapidly with distance from the sources due to coagulation and dilution.[84,85] The roadside average PNCs for this study are at least two times higher than those reported at European cities,[11] but an order of magnitude lower than other polluted Asian cities.[86–88]

The PMSD across all sites (Fig. 2b) shows bimodal distributions with peaks in the accumulation mode (185–234 nm) and coarse mode (2790–3318 nm) (Table S4†). Particles in the accumulation mode are the result of primary emissions (combustion particles like BC), gas-to-particle conversion (sulfate, ammonium, organics), and coagulation between particles.[66] A recent study at MO UB using size-segregated PM measurements showed that BC was more dominant in the accumulation mode, peaking between 180 and 320 nm.[25,31] Secondarily produced species (NH_4^+, SO_4^{2-}) peaked between 320 and 560 nm, while NO_3^- peaked between 1.8 and 3.2 μm.[25] Aside from NO_3^-, particles larger than 1 μm likely consist of non-exhaust traffic emissions, including resuspended road dust species like Al, Ca, Si, and Ti,[80] as well as particles from tire and metal brake wear enriched with Fe and Zn.[69]

A slight shift in PMSD was observed between the three sites (Fig. 2b). Compared with KAT RS, the accumulation mode at TAFT RS is slightly shifted towards the smaller size range, while the coarse mode is shifted towards the larger size range. At MO UB, particles in the accumulation mode shifted towards the larger size range; this is because particles changed in size when moving away from traffic due to coagulation.[84] The particles at MO UB are composed of more aged species compared to the freshly emitted particles at the roadside sites.

The mass concentration of UFPs ranged between 2.0 and 7.5 μg m^{-3} (7–18% of $PM_{2.5}$ mass) depending on the sampling site

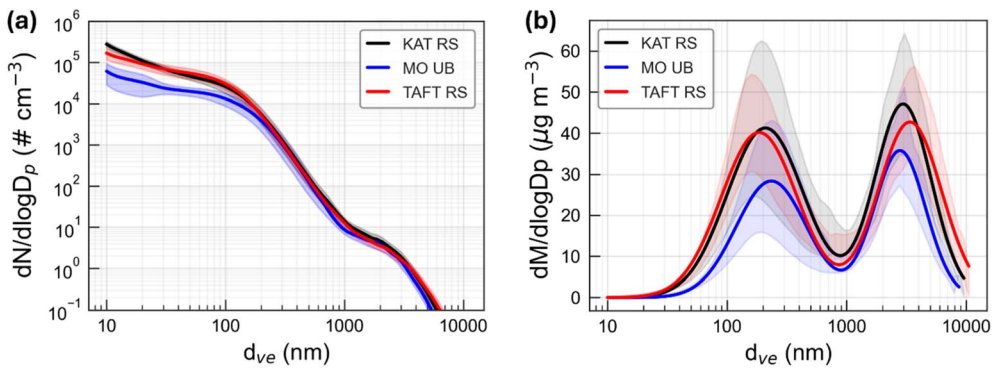

Fig. 2 Average (a) PNSD and (b) PMSD at KAT RS (black line), MO UB (blue line), and TAFT RS (red line) calculated from hourly data between 9 April–3 June 2015. The shaded area represents one standard deviation over the days sampled. d_{ve} represents volume equivalent diameter.

Table 2 Measured particle number concentrations (PNCs) (particle density: 1.8 g cm^{-3}) at KAT RS, MO UB, and TAFT RS for a specific size interval (size range units: nm), and number-derived mass concentration for those same size ranges

	KAT RS	MO UB	TAFT RS
(a) PNC (# cm^{-3})			
$N_{10–100}$	$9.6 \times 10^4 \pm 1.5 \times 10^4$	$2.9 \times 10^4 \pm 1.2 \times 10^4$	$7.7 \times 10^4 \pm 2.1 \times 10^4$
$N_{100–1000}$	$4.8 \times 10^3 \pm 1.8 \times 10^3$	$3.4 \times 10^3 \pm 1.3 \times 10^3$	$3.9 \times 10^3 \pm 1.1 \times 10^3$
$N_{1000–2500}$	7.0 ± 1.6	5.5 ± 1.3	4.8 ± 1.1
$N_{2500–10000}$	0.8 ± 0.2	0.6 ± 0.2	0.5 ± 0.1
$N_{10–100}/N_{10–2500}$	0.95	0.89	0.95
$N_{100–1000}/N_{10–2500}$	0.05	0.1	0.05
(b) Mass (μg m^{-3})			
$PM_{10–100}$	6.1 ± 1.4	2.0 ± 0.5	7.5 ± 2.0
$PM_{100–1000}$	28.5 ± 11.3	19.4 ± 8.8	25.4 ± 7.1
$PM_{1000–2500}$	9.4 ± 2.3	7.6 ± 2.0	8.5 ± 2.0
$PM_{2500–10000}$	16.9 ± 4.7	11.8 ± 3.3	17.6 ± 5.5
$PM_{10–100}/PM_{10–2500}$	0.14	0.07	0.18
$PM_{100–1000}/PM_{10–2500}$	0.65	0.67	0.61

(Table 2). For context, UFP mass concentrations in other Southeast Asian cities summarized in Phairuang *et al.*[16] ranged between 1.71 and 17.1 μg m^{-3} (Hanoi, Vietnam), 5.4–16.8 μg m^{-3} (different sites in Indonesia), 7.7–25.2 μg m^{-3} (Bangkok, Thailand), 18.9 μg m^{-3} (Phnom Phen, Cambodia), 9.3 μg m^{-3} (Kuala Lumpur, Malaysia), and 3.1 ± 0.91 μg m^{-3} (Sumatra, Indonesia).[89] In Delhi, India, UFP mass concentrations ranged between 2.1 and 10.3 μg m^{-3} (3–10% of $PM_{0.56}$) depending on season and time of day.[90] Other reported UFP mass concentrations in cleaner urban environments are as follows: <3 μg m^{-3} (Dresden, Germany),[91] <2 μg m^{-3} (Taipei, Taiwan),[92] and <0.2 μg m^{-3} (Los Angeles, East Oakland, San Pablo, and Fresno, California).[93] It is also clear in Table 2 that the particles in the accumulation mode have a substantial impact on particle mass, contributing as much as 61–67% to the number-derived $PM_{2.5}$ mass concentration.

Although UFP mass concentration was only 7–18% of the number-derived $PM_{2.5}$ mass, the UFP number concentration contributed as much as 89–95% within the 2.5 μm size range (Table 2). This result reveals that UFPs represent the highest share of the total number of particles at these sampling sites. This highlights the importance of long term particle number concentration measurements for health risk assessment studies.[94]

3.3 Mass closure

3.3.1 Gravimetric *versus* chemically-derived mass concentration. Aerosol chemical mass closure calculations were performed for the $PM_{2.5}$ aerosol collected at the three sites. Fig. 3 summarizes the contribution of the identified chemical species to the gravimetric $PM_{2.5}$ mass, which includes OM, EC, sulfate, nitrate, ammonium, crustal matter, and trace elements. As the chemical mass closure calculations require an estimation of OM contribution, OC was multiplied by a correction factor of 1.3 for the roadside sites and 1.4 for the urban mixed site as already noted in Section 2.5.2. OM accounted for 53.3% (MO UB), 51.9% (KAT RS), and 41.7% (TAFT RS) of the $PM_{2.5}$ mass concentration (Fig. 3). The contribution of OM at MO UB is nearly equal to the unaccounted $PM_{2.5}$ mass (52%) reported in Simpas *et al.*[28] for the same study site, suggesting that the unaccounted mass from the previous study was likely OM. For comparison, the OM contribution to $PM_{2.5}$ mass in other studies in Asia are as follows: 33.3% (roadside: Delhi, India);[95] 42% (kerb site: Mumbai, India);[75] 35% (urban background: Europe);[96] 27% (roadside: Hongkong);[97] and 14% (urban area: Jinan City, China).[98]

EC contributed the most to $PM_{2.5}$ at TAFT RS (47.9%), followed by KAT RS (35.8%), and MO UB (18.7%). For the same measurement campaign, Kecorius *et al.*[26] reported that eBC in Manila contributed 55–75% to total $PM_{2.5}$ mass. Compared with EC, the measured BC *via* reflectometry at TAFT RS contributed to 50–71% of the total $PM_{2.5}$ mass, which is near the measured value reported by Kecorius *et al.*[26] Overall, BC levels for this study were on average 20% higher than EC, which is close to the 17.39% obtained by Salako *et al.*[99] who studied the variability between EC and BC at different locations in Asia and the South Pacific. At MO UB, since the site was only 350 m away from the main road, Katipunan traffic is expected to influence the measured BC especially when it was downwind of Katipunan. Furthermore, MO UB was also impacted by the exhaust from vehicles coming in and out of the ADMU campus. However, because the school calendar shift coincided with the campaign period, we expected reduced traffic both on-campus and main road, and consequently less EC.

Secondary inorganic aerosols (sum of sulfate, nitrate, and ammonium) accounted for 9.5% (KAT RS), 14.4% (MO UB), and 9.8% (TAFT RS) of the total $PM_{2.5}$ mass. The higher percentage of secondarily produced aerosol at MO UB is suggestive that the air masses transported in the area were more aged as compared to the roadside site's more freshly emitted particles. Contribution of crustal species and trace elements were 5.6 and 1.2% (KAT RS), 5.9 and 1.3% (MO UB), and 3.9 and 0.7% (TAFT RS), respectively. Sea salt accounted for less than 1% of the total PM mass at the three sites.

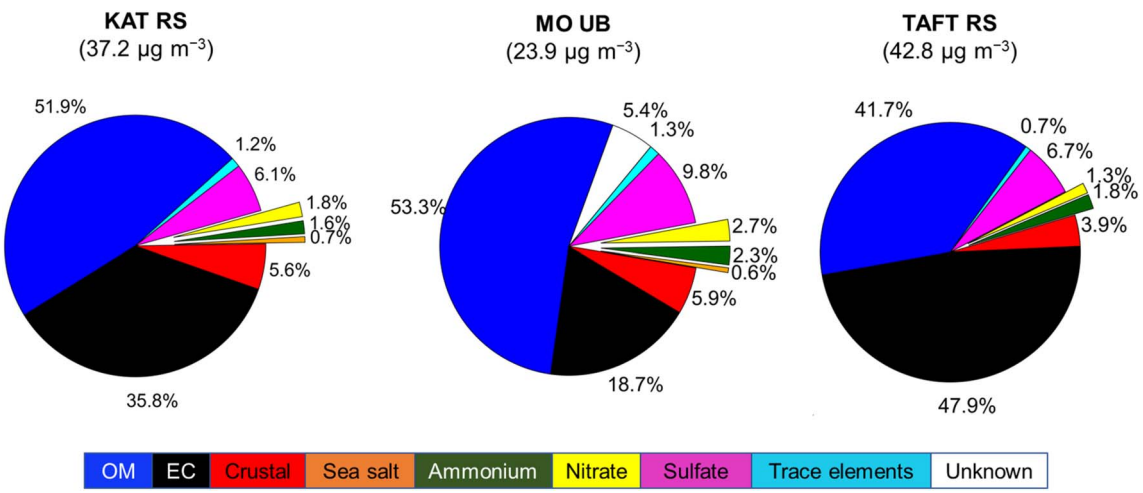

Fig. 3 Average speciated breakdown (in percentage) of the $PM_{2.5}$ gravimetric mass concentration at individual sites. Total mass concentration is shown at the top of each pie chart.

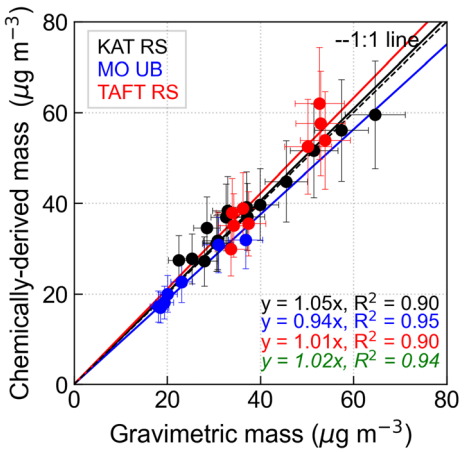

Fig. 4 Linear regression analysis of the gravimetric mass *versus* chemically-derived mass for KAT RS (black line), MO UB (blue line), and TAFT RS (red line) with the 1 : 1 line shown as a black dashed line. The linear equation statistics correspond to sites based on color, where the italicized equation (in green) is for all data. The error bars for the chemically-derived mass concentrations were taken to be ±20%. For the gravimetric mass, an error value of ±10% was used.

The sums of all the included chemical species to total $PM_{2.5}$ mass were 104% for the two roadside sites, and 95% for the urban mixed site. The measured $PM_{2.5}$ mass accounted for in other closure studies are as follows: 115% (traffic area: Delhi, India);[95] 79–106% (six urban background sites: Europe);[96] 75% (urban site: Athens, Greece);[46] 98% (roadside: Hongkong).[97] Although the closure was quite close to 100%, potential sources of uncertainty and/or reasons for the slight over- and under-estimation were possibly due to: (i) adsorption of volatile organic carbons on quartz filters;[100,101] (ii) use of a fixed OC multiplier for the quantification of the OM contribution;[96] (iii) conversion factors for the crustal elements and; (iv) volatilization during and after sample collection.[101] To assess sensitivity of closure to different conversion factors, we varied OM : OC ratios from 1.1 to 2.0.[50] By looking at the difference between the sum of the identified chemical components and the gravimetric mass, the upper limit of the OM : OC ratio can be estimated.[102] At the MO UB site, the OM : OC upper limit was 1.6, whereas in the KAT RS and TAFT RS an OM : OC ratio upper limit of 1.2 was obtained. Our use of 1.3 conversion factor in the roadside sites resulted in an overestimation of approximately 5% while our use of 1.4 in the MO UB site resulted in an underestimation of around 5%. Overall, linear regression between gravimetric mass and chemically-derived mass showed excellent correlation (r^2 = 0.94) indicating a well-explained total $PM_{2.5}$ mass (Fig. 4).

3.3.2 Gravimetric *versus* number-derived mass concentration. The PMSD was derived from the merged MPSS and APSS data. From the single PMSD, the hourly number-derived mass

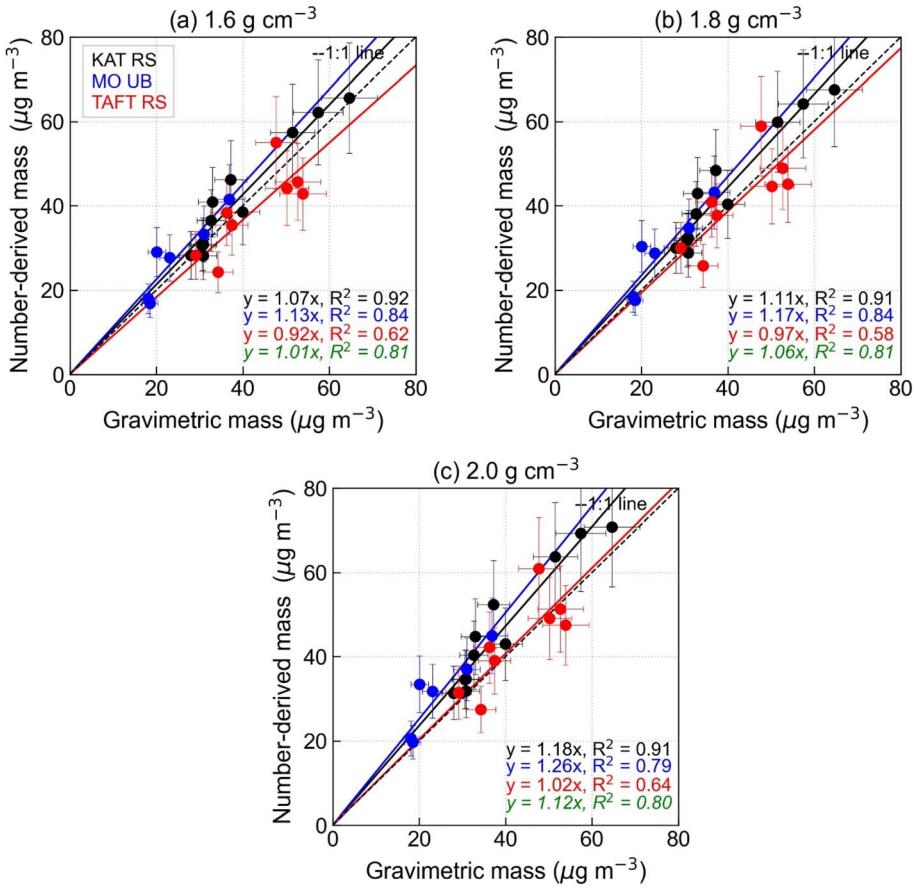

Fig. 5 Same as Fig. 4 except for comparing gravimetric mass *versus* number-derived mass for (a–c) different assumed particle densities.

concentration of $PM_{2.5}$ was calculated, which was then summed daily for comparison with the $PM_{2.5}$ gravimetric mass concentration. Sources of uncertainties for this method may include: (i) instruments' concentration and sizing errors, which may contribute up to 10% of the uncertainty;[58,103] (ii) inversion routine, which provides 5% deviation with respect to the resulting PNSD[58] and; (iii) assumed particle density used to convert the aerodynamic diameter to Stokes diameter, which is estimated to have a systematic error of 5–10%.[104]

Since measurements of particle density are non-existent in Metro Manila, we based the particle density used in the inversion algorithm on prior studies of PM chemical composition in the study area.[25,28] A constant particle density (1.8 g cm^{-3}) was used for this study. An uncertainty of ±20% was adopted from Khlystov *et al.*[10] and was incorporated into the daily number-derived mass concentration (Fig. 5). The estimated uncertainty is due to both the changes in aerosol composition (density change) as well as the aerosol shape.[105] For this study, the majority of the sampling days have number-derived mass with ±20% uncertainty. The use of constant particle density resulted in an under- and over-estimation of the daily number-derived mass concentration as particle density varies day-to-day.[7,104] For individual sites, on average, the number-derived mass overestimated the gravimetric mass at KAT RS (slope = 1.11, r^2 = 0.91) and MO UB (slope = 1.17, r^2 = 0.84), while underestimating gravimetric mass at TAFT RS (slope = 0.97, r^2 = 0.58). Combining samples from all sites, the linear regression analysis revealed a strong correlation between the number-derived mass and gravimetric mass concentration (slope = 1.06, r^2 = 0.81) (Fig. 5b). This value exhibits excellent agreement with values obtained from other mass closure studies.[59,104] On average, the estimated mass from the combined MPSS + APSS was 6% higher than the gravimetric mass.

To determine the best value of the input density parameter, aside from 1.8 g cm^{-3}, we also explored two other particle density values (1.6 g cm^{-3} and 2.0 g cm^{-3}) in fitting the MPSS and APSS PNSDs. The use of 1.6 g cm^{-3} particle density improved the mass closure at KAT RS and MO UB, while the use of 2.0 g cm^{-3} improved the closure at TAFT RS (Fig. 5a and c). This result suggests that a particle density of 2.0 g cm^{-3} may be more appropriate to use at TAFT RS due to larger contribution of EC at this site compared to KAT RS and MO UB where OM was more dominant.

4 Conclusions

In this study, we comprehensively characterize the chemical composition, as well as the physical properties of $PM_{2.5}$ obtained from the three different sampling sites in Metro Manila. Our results showed that the major components in $PM_{2.5}$ mass at MO UB, KAT RS, and TAFT RS are organic matter (53.3, 51.9, 41.7%), elemental carbon (18.7, 35.8, 47.9%), secondary inorganic aerosols (14.4, 9.5, 9.8%), crustal matter (5.9, 5.6, 3.9%), and trace elements (1.3, 1.2, 0.7%), respectively.

The average OC/EC ratios at the roadside sites suggest freshly emitted aerosols (soot) from traffic sources, while the ratio exceeding 2 at the urban mixed site points to more aged aerosols associated with secondary organic carbon (SOC) formation. Consistently, the estimated SOC contribution was highest at MO UB (52%), followed by KAT RS (38%) and TAFT RS (28%), reinforcing the influence of secondary formation processes at the urban mixed site compared to the traffic-dominated roadside sites.

The PNCs measured at the roadside sites ($8.1 \times 10^4 - 1 \times 10^5$ cm^{-3}) are at least two times higher than at the urban mixed site (3.2×10^4 cm^{-3}). The ultrafine particles make up the majority of the total particle number concentration (89–95%); however, they only accounted for 7–18% of the number-derived $PM_{2.5}$ mass. Unlike UFPs, particles in the accumulation mode contributes as much as 61–67% of the total $PM_{2.5}$ mass.

Results of mass closure reveal that the chemically-derived mass agreed well with the gravimetric mass (slope = 1.02; r^2 = 0.94). The identified chemical components accounted for 95% at the urban mixed site and 104% at both the roadside sites. The over- and under-estimation was largely attributed to the use of conversion factors, especially the OC-to-OM conversion factor. The number-derived $PM_{2.5}$ mass concentration also correlated well with gravimetric mass (slope = 1.06; r^2 = 0.81). The over- and under-estimation for this method was possibly due to measurement uncertainties and assumptions, especially the use of assumed particle density in the inversion routine. Overall, mass closure was achieved, and our method can be used to quantify the PM mass concentration using the continuous PNSD measurement.

The high fraction of carbonaceous and combustion particles makes it pivotal to control the corresponding sources if PM pollution is to be significantly reduced in the Metro Manila area. Our results also suggest investigating not only the mass concentration but also the number concentration as the latter is also relevant for epidemiological studies and studies of cloud microphysics that are concerned more with number concentrations of aerosol particles and cloud droplets. Greater emphasis on measuring the chemical and number concentrations of UFPs, as well as assessing the health risks associated with UFP-bound toxic carbon and trace elements,[106,107] should be prioritized in future studies. This study provides an incremental and valuable contribution to the understanding of the atmospheric composition of an emerging megacity in Southeast Asia and serves as an important input to the development of air pollution mitigation strategies, as well as for future epidemiological studies, which are still lacking in this region.

Data availability

The datasets used in this manuscript are accessible at **https://doi.org/10.5281/zenodo.14913715**. HYSPLIT data are available through the NOAA READY website (**http://www.ready.noaa.gov**).

Author contributions

GB and GC-J conducted the data analysis and drafted the original manuscript. All other authors contributed to the campaign design, funding acquisition, measurement phase, and the

discussion, review, and editing of the manuscript. All authors have approved the final version of the manuscript.

Conflicts of interest

There are no conflicts to declare.

Acknowledgements

This research was supported by the Researchers for Clean Air, Inc., and the Leibniz-Institut für Troposphärenforschung e.V. (TROPOS). This research was also partly funded by the German Federal Ministry of Education and Research in the framework of TAME-BC (project number 01LE1903A). Funding for the ion chromatography (IC) analysis was provided by the ADMU Research Council Grant No. 16-13. We would like to acknowledge the DOST-PNRI for allowing us to use their IC system for the water-soluble ion analysis. G. Betito and G. Catipay-Jamero acknowledge support from the DOST-Accelerated Science and Technology Human Resource Development Program (ASTHRDP) scholarship. A. Sorooshian was supported by NASA grant 80NSSC18K0148 in support of CAMP^{2}Ex. The authors acknowledge the NOAA Air Resources Laboratory (ARL) for the provision of the HYSPLIT transport and dispersion model and READY website (**https://www.ready.noaa.gov**) used in this publication. We thank Connor Stahl for providing feedback on the initial draft of this paper. Special thank you to Jackie Ibañez who participated in $PM_{2.5}$ measurements throughout the campaign.

References

1 N. M. Johnson, A. R. Hoffmann, J. C. Behlen, C. Lau, D. Pendleton, N. Harvey, R. Shore, Y. Li, J. Chen, Y. Tian and R. Zhang, Air pollution and children's health-a review of adverse effects associated with prenatal exposure from fine to ultrafine particulate matter, *Environ. Health Prev. Med.*, 2021, **26**, 72.

2 N. P. Hyslop, Impaired visibility: the air pollution people see, *Atmos. Environ.*, 2009, **43**, 182–195.

3 A. Roy, M. Mandal, S. Das, R. Popek, R. Rakwal, G. K. Agrawal, A. Awasthi and A. Sarkar, The cellular consequences of particulate matter pollutants in plants: Safeguarding the harmonious integration of structure and function, *Sci. Total Environ.*, 2024, **914**, 169763.

4 S.-L. Chen, S.-W. Chang, Y.-J. Chen and H.-L. Chen, Possible warming effect of fine particulate matter in the atmosphere, *Commun. Earth Environ.*, 2021, **2**, 208.

5 C. Pope, R. Burnett, M. Thun, E. Calle, D. Krewski, K. Ito and G. Thurston, Lung cancer, cardiopulmonary mortality, and long-term exposure to fine particulate air pollution, *J. Am. Med. Assoc.*, 2002, **287**, 1132–1141.

6 S. Sangkham, W. Phairuang, S. P. Sherchan, N. Pansakun, N. Munkong, K. Sarndhong, M. A. Islam and P. Sakunkoo, An update on adverse health effects from exposure to PM2.5, *Environ. Adv.*, 2024, **18**, 100603.

7 M. Pitz, O. Schmid, J. Heinrich, W. Birmili, J. Maguhn, R. Zimmerman, H.-E. Wichmann, A. Peters and J. Cyrys, Seasonal and Diurnal Variation of PM2.5 Apparent Particle Density in Urban Air in Augsburg, Germany, *Environ. Sci. Technol.*, 2008, **42**, 5087–5093.

8 S. Ridolfo, F. Amato and X. Querol, Particle number size distributions and concentrations in transportation environments: a review, *Environ. Int.*, 2024, **187**, 108696.

9 P. H. McMurry, X. Wang, K. Park and K. Ehara, The Relationship between Mass and Mobility for Atmospheric Particles: A New Technique for Measuring Particle Density, *Aerosol Sci. Technol.*, 2002, **36**, 227–238.

10 A. Khlystov, C. Stanier and S. N. Pandis, An Algorithm for Combining Electrical Mobility and Aerodynamic Size Distributions Data when Measuring Ambient Aerosol Special Issue ofAerosol Science and Technologyon Findings from the Fine Particulate Matter Supersites Program, *Aerosol Sci. Technol.*, 2004, **38**, 229–238.

11 L. Morawska, Z. Ristovski, E. R. Jayaratne, D. U. Keogh and X. Ling, Ambient nano and ultrafine particles from motor vehicle emissions: Characteristics, ambient processing and implications on human exposure, *Atmos. Environ.*, 2008, **42**, 8113–8138.

12 M. Geller, S. Biswas and C. Sioutas, Determination of Particle Effective Density in Urban Environments with a Differential Mobility Analyzer and Aerosol Particle Mass Analyzer, *Aerosol Sci. Technol.*, 2006, **40**, 709–723.

13 M. Pitz, J. Cyrys, E. Karg, A. Wiedensohler, H. E. Wichmann and J. Heinrich, Variability of apparent particle density of an urban aerosol, *Environ. Sci. Technol.*, 2003, **37**, 4336–4342.

14 J. P. Putaud, R. Van Dingenen, A. Alastuey, H. Bauer, W. Birmili, J. Cyrys, H. Flentje, S. Fuzzi, R. Gehrig, H. C. Hansson, R. M. Harrison, H. Herrmann, R. Hitzenberger, C. Hüglin, A. M. Jones, A. Kasper-Giebl, G. Kiss, A. Kousa, T. A. J. Kuhlbusch, G. Löschau, W. Maenhaut, A. Molnar, T. Moreno, J. Pekkanen, C. Perrino, M. Pitz, H. Puxbaum, X. Querol, S. Rodriguez, I. Salma, J. Schwarz, J. Smolik, J. Schneider, G. Spindler, H. ten Brink, J. Tursic, M. Viana, A. Wiedensohler and F. Raes, A European aerosol phenomenology – 3: Physical and chemical characteristics of particulate matter from 60 rural, urban, and kerbside sites across Europe, *Atmos. Environ.*, 2010, **44**, 1308–1320.

15 W. Phairuang, S. Piriyakarnsakul, M. Inerb, S. Hongtieab, T. Thongyen, J. Chomanee, Y. Boongla, P. Suriyawong, H. Samae, P. Chanonmuang, P. Suwattiga, T. Chetiyanukornkul, S. Panyametheekul, M. Amin, M. Hata and M. Furuuchi, Ambient Nanoparticles (PM0.1) Mapping in Thailand, *Atmosphere*, 2022, **14**, 66.

16 W. Phairuang, M. Amin, M. Hata and M. Furuuchi, Airborne Nanoparticles (PM0.1) in Southeast Asian Cities: A Review, *Sustainability*, 2022, **14**, 10074.

17 K. Park, F. Cao, D. B. Kittelson and P. H. McMurry, Relationship between particle mass and mobility for diesel exhaust particles, *Environ. Sci. Technol.*, 2003, **37**, 577–583.

18 T. Hussein, A. Puustinen, P. P. Aalto, J. M. Makela, K. Hameri and M. Kulmala, Urban aerosol number size distributions, *Atmos. Chem. Phys.*, 2004, **4**, 391–411.
19 R. M. Harrison, J. P. Shi, S. Xi, A. Khan, D. Mark, R. Kinnersley and J. Yin, Measurement of number, mass and size distribution of particles in the atmosphere, *Philos. Trans. R. Soc. London, Ser. A*, 2000, **358**, 2567–2580.
20 M. Schwarz, A. Schneider, J. Cyrys, S. Bastian, S. Breitner and A. Peters, Impact of ultrafine particles and total particle number concentration on five cause-specific hospital admission endpoints in three German cities, *Environ. Int.*, 2023, **178**, 108032.
21 G. Oberdörster, E. Oberdörster and J. Oberdörster, Nanotoxicology: An emerging discipline evolving from studies of ultrafine particles, *Environ. Health Perspect.*, 2005, **113**, 823–839.
22 M. Amin, S. Aun, C. Or, M. Hata, W. Phairuang, A. Toriba and M. Furuuchi, Characterization of carbonaceous components and PAHs on ultrafine particles in Phnom Penh, Cambodia, *Environ. Monit. Assess.*, 2024, **196**, 895.
23 W. Phairuang, S. Hongtieab, P. Suwattiga, M. Furuuchi and M. Hata, Atmospheric Ultrafine Particulate Matter (PM0.1)-Bound Carbon Composition in Bangkok, Thailand, *Atmosphere*, 2022, **13**, 1676.
24 D. D. Cohen, E. Stelcer, F. L. Santos, M. Prior, C. Thompson and P. C. B. Pabroa, Fingerprinting and source apportionment of fine particle pollution in Manila by IBA and PMF techniques: A 7-year study, *X-Ray Spectrom.*, 2008, **38**, 18–25.
25 M. T. Cruz, P. A. Bañaga, G. Betito, R. A. Braun, C. Stahl, M. A. Aghdam, M. O. Cambaliza, H. Dadashazar, M. R. Hilario, G. R. Lorenzo, L. Ma, A. B. MacDonald, P. C. Pabroa, J. R. Yee, J. B. Simpas and A. Sorooshian, Size-resolved composition and morphology of particulate matter during the southwest monsoon in Metro Manila, Philippines, *Atmos. Chem. Phys.*, 2019, **19**, 10675–10696.
26 S. Kecorius, L. Madueño, E. Vallar, H. Alas, G. Betito, W. Birmili, M. O. Cambaliza, G. Catipay, M. Gonzaga-Cayetano, M. C. Galvez, G. Lorenzo, T. Müller, J. B. Simpas, E. G. Tamayo and A. Wiedensohler, Aerosol particle mixing state, refractory particle number size distributions and emission factors in a polluted urban environment: Case study of Metro Manila, Philippines, *Atmos. Environ.*, 2017, **170**, 169–183.
27 R. A. Braun, M. A. Aghdam, P. A. Bañaga, G. Betito, M. O. Cambaliza, M. T. Cruz, G. R. Lorenzo, A. B. MacDonald, J. B. Simpas, C. Stahl and A. Sorooshian, Long-range aerosol transport and impacts on size-resolved aerosol composition in Metro Manila, Philippines, *Atmos. Chem. Phys.*, 2020, **20**, 2387–2405.
28 J. Simpas, G. Lorenzo and M. T. Cruz, in *Improving Air Quality in Asian Developing Countries: Compilation of Research Finding*, ed. N. T. Kim Oanh, Vietnam Publishing House of Natural Resources, Environment and Cartography, Vietnam, 2014, ch. 13, pp. 239–261.
29 P. K. Hopke, D. D. Cohen, B. A. Begum, S. K. Biswas, B. Ni, G. G. Pandit, M. Santoso, Y. S. Chung, S. A. Rahman, M. S. Hamzah, P. Davy, A. Markwitz, S. Waheed, N. Siddique, F. L. Santos, P. C. Pabroa, M. C. Seneviratne, W. Wimolwattanapun, S. Bunprapob, T. B. Vuong, P. Duy Hien and A. Markowicz, Urban air quality in the Asian region, *Sci. Total Environ.*, 2008, **404**, 103–112.
30 N. T. Kim Oanh, N. Upadhyay, Y. H. Zhuang, Z. P. Hao, D. V. S. Murthy, P. Lestari, J. T. Villarin, K. Chengchua, H. X. Co and N. T. Dung, Particulate air pollution in six Asian cities: Spatial and temporal distributions, and associated sources, *Atmos. Environ.*, 2006, **40**, 3367–3380.
31 M. R. A. Hilario, M. T. Cruz, P. A. Bañaga, G. Betito, R. A. Braun, C. Stahl, M. O. Cambaliza, G. R. Lorenzo, A. B. MacDonald, M. AzadiAghdam, P. C. Pabroa, J. R. Yee, J. B. Simpas and A. Sorooshian, Characterizing Weekly Cycles of Particulate Matter in a Coastal Megacity: The Importance of a Seasonal, Size-Resolved, and Chemically Speciated Analysis, *J. Geophys. Res.: Atmos.*, 2020, **125**, e2020JD032614.
32 P. C. B. Pabroa, J. M. D. Racho, A. M. Jagonoy, J. D. G. Valdez, A. T. Bautista Vii, J. R. Yee, R. Pineda, J. Manlapaz, A. J. Atanacio, I. C. V. Coronel, C. M. G. Salvador and D. D. Cohen, Characterization, source apportionment and associated health risk assessment of respirable air particulates in Metro Manila, Philippines, *Atmos. Pollut. Res.*, 2022, **13**, 101379.
33 A. Petzold, J. A. Ogren, M. Fiebig, P. Laj, S. M. Li, U. Baltensperger, T. Holzer-Popp, S. Kinne, G. Pappalardo, N. Sugimoto, C. Wehrli, A. Wiedensohler and X. Y. Zhang, Recommendations for reporting "black carbon" measurements, *Atmos. Chem. Phys.*, 2013, **13**, 8365–8379.
34 H. D. Alas, T. Müller, W. Birmili, S. Kecorius, M. O. Cambaliza, J. B. B. Simpas, M. Cayetano, K. Weinhold, E. Vallar, M. C. Galvez and A. Wiedensohler, Spatial Characterization of Black Carbon Mass Concentration in the Atmosphere of a Southeast Asian Megacity: An Air Quality Case Study for Metro Manila, Philippines, *Aerosol Air Qual. Res.*, 2018, **18**, 2301–2317.
35 B. Guinot, H. Cachier and K. Oikonomou, Geochemical perspectives from a new aerosol chemical mass closure, *Atmos. Chem. Phys.*, 2007, **7**, 1657–1670.
36 L. Li, W. Wang, J. Feng, D. Zhang, H. Li, Z. Gu, B. Wang, G. Sheng and J. Fu, Composition, source, mass closure of PM2.5 aerosols for four forests in eastern China, *J. Environ. Sci.*, 2010, **22**, 405–412.
37 E. Terzi, G. Argyropoulos, A. Bougatioti, N. Mihalopoulos, K. Nikolaou and C. Samara, Chemical composition and mass closure of ambient PM10 at urban sites, *Atmos. Environ.*, 2010, **44**, 2231–2239.
38 J. T. Collado, J. G. Abalos, I. de los Reyes, M. T. Cruz, G. F. Leung, K. Abenojar, C. R. Manalo, B. Go, C. L. Chan, C. K. G. Gonzales, J. B. B. Simpas, E. E. Porio, J. Q. Wong, S.-C. C. Lung and M. O. L. Cambaliza, Spatiotemporal Assessment of PM2.5 Exposure of a High-risk Occupational Group in a Southeast Asian Megacity, *Aerosol Air Qual. Res.*, 2023, **23**, 220134.

39 G. Rolph, A. Stein and B. Stunder, Real-time Environmental Applications and Display sYstem: READY, *Environ. Model. Software*, 2017, **95**, 210–228.
40 A. F. Stein, R. R. Draxler, G. D. Rolph, B. J. B. Stunder, M. D. Cohen and F. Ngan, NOAA's HYSPLIT Atmospheric Transport and Dispersion Modeling System, *Bull. Am. Meteorol. Soc.*, 2015, **96**, 2059–2077.
41 A. Wiedensohler, W. Birmili, A. Nowak, A. Sonntag, K. Weinhold, M. Merkel, B. Wehner, T. Tuch, S. Pfeifer, M. Fiebig, A. M. Fjäraa, E. Asmi, K. Sellegri, R. Depuy, H. Venzac, P. Villani, P. Laj, P. Aalto, J. A. Ogren, E. Swietlicki, P. Williams, P. Roldin, P. Quincey, C. Hüglin, R. Fierz-Schmidhauser, M. Gysel, E. Weingartner, F. Riccobono, S. Santos, C. Grüning, K. Faloon, D. Beddows, R. Harrison, C. Monahan, S. G. Jennings, C. D. O'Dowd, A. Marinoni, H. G. Horn, L. Keck, J. Jiang, J. Scheckman, P. H. McMurry, Z. Deng, C. S. Zhao, M. Moerman, B. Henzing, G. de Leeuw, G. Löschau and S. Bastian, Mobility particle size spectrometers: harmonization of technical standards and data structure to facilitate high quality long-term observations of atmospheric particle number size distributions, *Atmos. Meas. Tech.*, 2012, **5**, 657–685.
42 A. T. Bautista, P. C. B. Pabroa, F. L. Santos, J. M. D. Racho and L. L. Quirit, Carbonaceous particulate matter characterization in an urban and a rural site in the Philippines, *Atmos. Pollut. Res.*, 2014, **5**, 245–252.
43 J. C. Chow, J. G. Watson, L. W. Chen, M. C. Chang, N. F. Robinson, D. Trimble and S. Kohl, The IMPROVE_A temperature protocol for thermal/optical carbon analysis: maintaining consistency with a long-term database, *J. Air Waste Manag. Assoc.*, 2007, **57**, 1014–1023.
44 C. Stahl, M. T. Cruz, P. A. Banaga, G. Betito, R. A. Braun, M. A. Aghdam, M. O. Cambaliza, G. R. Lorenzo, A. B. MacDonald, P. C. Pabroa, J. R. Yee, J. B. Simpas and A. Sorooshian, An annual time series of weekly size-resolved aerosol properties in the megacity of Metro Manila, Philippines, *Sci. Data*, 2020, **7**, 128.
45 C. Perrino, M. Catrambone, C. Farao, R. Salzano, G. Esposito, M. Giusto, M. Montagnoli, A. Marini, M. Brinoni, G. Simonetti and S. Canepari, Improved Time-Resolved Measurements of Inorganic Ions in Particulate Matter by PILS-IC Integrated with a Sample Pre-Concentration System, *Aerosol Sci. Technol.*, 2015, **49**, 521–530.
46 E. Remoundaki, P. Kassomenos, E. Mantas, N. Mihalopoulos and M. Tsezos, Composition and Mass Closure of PM2.5 in Urban Environment (Athens, Greece), *Aerosol Air Qual. Res.*, 2013, **13**, 72–82.
47 J. Gao, H. Tian, K. Cheng, L. Lu, M. Zheng, S. Wang, J. Hao, K. Wang, S. Hua, C. Zhu and Y. Wang, The variation of chemical characteristics of PM2.5 and PM10 and formation causes during two haze pollution events in urban Beijing, China, *Atmos. Environ.*, 2015, **107**, 1–8.
48 D. Liu, Y. Su, H. Peng, W. Yan, Y. Li, X. Liu, B. Zhu, H. Wang and X. Zhang, Size Distributions of Water-soluble Inorganic Ions in Atmospheric Aerosols during the Meiyu Period on the North Shore of Taihu Lake, China, *Aerosol Air Qual. Res.*, 2018, **18**, 2997–3008.
49 D. D. Cohen, *The IAEA/RCA fine and coarse particle ambient air database*, Australian Nuclear Science and Technology Organisation, Lucas Heights, NSW, 2010, **http://apo.ansto.gov.au/dspace/handle/10238/6404.Journal**.
50 B. J. Turpin and H.-J. Lim, Species Contributions to PM2.5 Mass Concentrations: Revisiting Common Assumptions for Estimating Organic Mass, *Aerosol Sci. Technol.*, 2001, **35**, 602–610.
51 L. M. Russell, Aerosol Organic-Mass-to-Organic Carbon Ratio Measurements, *Environ. Sci. Technol.*, 2003, **37**, 2982–2987.
52 A. M. Taiwo, Source Apportionment of Urban Background Particulate Matter in Birmingham, United Kingdom Using a Mass Closure Model, *Aerosol Air Qual. Res.*, 2016, **16**, 1244–1252.
53 J. Brito, L. V. Rizzo, P. Herckes, P. C. Vasconcellos, S. E. S. Caumo, A. Fornaro, R. Y. Ynoue, P. Artaxo and M. F. Andrade, Physical–chemical characterisation of the particulate matter inside two road tunnels in the São Paulo Metropolitan Area, *Atmos. Chem. Phys.*, 2013, **13**, 12199–12213.
54 W. H. White, Chemical markers for sea salt in IMPROVE aerosol data, *Atmos. Environ.*, 2008, **42**, 261–274.
55 W. C. Malm, B. A. Schichtel, M. L. Pitchford, L. L. Ashbaugh and R. A. Eldred, Spatial and monthly trends in speciated fine particle concentration in the United States, *J. Geophys. Res.: Atmos.*, 2004, **109**, D03306.
56 J. C. Chow, J. G. Watson, Z. Lu, D. H. Lowenthal, C. A. Frazier, P. A. Solomon, R. H. Thuellier and K. Magliano, Descriptive Analysis of PM2.5 and PM10 at Regionally Representative Locations During SJVAQS/AUSPEX, *Atmos. Environ.*, 1996, **30**, 2079–2112.
57 P. A. Solomon, T. Fall, L. Salmon, G. R. Cass, H. A. Gray and A. Davidson, Chemical Characteristics of PM10Aerosols Collected in the Los Angeles Area, *Japca*, 1989, **39**, 154–163.
58 S. Pfeifer, W. Birmili, A. Schladitz, T. Müller, A. Nowak and A. Wiedensohler, A fast and easy-to-implement inversion algorithm for mobility particle size spectrometers considering particle number size distribution information outside of the detection range, *Atmos. Meas. Tech.*, 2014, **7**, 95–105.
59 D. C. S. Beddows, M. Dall'osto and R. M. Harrison, An Enhanced Procedure for the Merging of Atmospheric Particle Size Distribution Data Measured Using Electrical Mobility and Time-of-Flight Analysers, *Aerosol Sci. Technol.*, 2010, **44**, 930–938.
60 F. Tavakoli and J. S. Olfert, Determination of particle mass, effective density, mass–mobility exponent, and dynamic shape factor using an aerodynamic aerosol classifier and a differential mobility analyzer in tandem, *J. Aerosol Sci.*, 2014, **75**, 35–42.
61 J. G. Slowik, K. Stainken, P. Davidovits, L. R. Williams, J. T. Jayne, C. E. Kolb, D. R. Worsnop, Y. Rudich, P. F. DeCarlo and J. L. Jimenez, Particle Morphology and Density Characterization by Combined Mobility and

Aerodynamic Diameter Measurements. Part 2: Application to Combustion-Generated Soot Aerosols as a Function of Fuel Equivalence Ratio, *Aerosol Sci. Technol.*, 2004, **38**, 1206–1222.

62 G. Buonanno, M. Dell'Isola, L. Stabile and A. Viola, Uncertainty Budget of the SMPS–APS System in the Measurement of PM1, PM2.5, and PM10, *Aerosol Sci. Technol.*, 2009, **43**, 1130–1141.

63 G. Bagtasa, M. G. Cayetano and C.-S. Yuan, Seasonal variation and chemical characterization of PM2.5 in northwestern Philippines, *Atmos. Chem. Phys.*, 2018, **18**, 4965–4980.

64 B. Zeb, K. Alam, A. Sorooshian, T. Blaschke, I. Ahmad and I. Shahid, On the Morphology and Composition of Particulate Matter in an Urban Environment, *Aerosol Air Qual. Res.*, 2018, **18**, 1431–1447.

65 X. Querol, A. Alastuey, M. Viana, T. Moreno, C. Reche, M. C. Minguillón, A. Ripoll, M. Pandolfi, F. Amato, A. Karanasiou, N. Pérez, J. Pey, M. Cusack, R. Vázquez, F. Plana, M. Dall'Osto, J. de la Rosa, A. Sánchez de la Campa, R. Fernández-Camacho, S. Rodríguez, C. Pio, L. Alados-Arboledas, G. Titos, B. Artíñano, P. Salvador, S. García Dos Santos and R. Fernández Patier, Variability of carbonaceous aerosols in remote, rural, urban and industrial environments in Spain: implications for air quality policy, *Atmos. Chem. Phys.*, 2013, **13**, 6185–6206.

66 J. H. Seinfeld and S. N. Pandis, *Atmospheric Chemistry and Physics: from Air Pollution to Climate Change*, John Wiley & Sons, Hoboken, 3rd edn, 2016.

67 S. Saarikoski, H. Timonen, K. Saarnio, M. Aurela, L. Jarvi, P. Keronen, V.-M. Kerminen and R. Hillamo, Sources of organic carbon in fine particulate matter in northern European urban air, *Atmos. Chem. Phys.*, 2008, **8**, 6281–6295.

68 P. Lestari and Y. D. Mauliadi, Source apportionment of particulate matter at urban mixed site in Indonesia using PMF, *Atmos. Environ.*, 2009, **43**, 1760–1770.

69 L. Yao, L. Yang, Q. Yuan, C. Yan, C. Dong, C. Meng, X. Sui, F. Yang, Y. Lu and W. Wang, Sources apportionment of PM2.5 in a background site in the North China Plain, *Sci. Total Environ.*, 2016, **541**, 590–598.

70 A. Genga, P. Ielpo, T. Siciliano and M. Siciliano, Carbonaceous particles and aerosol mass closure in PM2.5 collected in a port city, *Atmos. Res.*, 2017, **183**, 245–254.

71 O. V. Rattigan, H. Dirk Felton, M.-S. Bae, J. J. Schwab and K. L. Demerjian, Multi-year hourly PM2.5 carbon measurements in New York: Diurnal, day of week and seasonal patterns, *Atmos. Environ.*, 2010, **44**, 2043–2053.

72 C. Pio, M. Cerqueira, R. M. Harrison, T. Nunes, F. Mirante, C. Alves, C. Oliveira, A. Sanchez de la Campa, B. Artíñano and M. Matos, OC/EC ratio observations in Europe: Re-thinking the approach for apportionment between primary and secondary organic carbon, *Atmos. Environ.*, 2011, **45**, 6121–6132.

73 B. Ervens, A. Sorooshian, A. M. Aldhaif, T. Shingler, E. Crosbie, L. Ziemba, P. Campuzano-Jost, J. L. Jimenez and A. Wisthaler, Is there an aerosol signature of chemical cloud processing?, *Atmos. Chem. Phys.*, 2018, **18**, 16099–16119.

74 L. M. Castro, C. A. Pio, R. M. Harrison and D. J. T. Smith, Carbonaceous aerosol in urban and rural European atmospheres: estimation of secondary organic carbon concentrations, *Atmos. Environ.*, 1999, **33**, 2771–2781.

75 A. E. Joseph, S. Unnikrishnan and R. Kumar, Chemical Characterization and Mass Closure of Fine Aerosol for Different Land Use Patterns in Mumbai City, *Aerosol Air Qual. Res.*, 2012, **12**, 61–72.

76 Z. Ramadan, X. H. Song and P. K. Hopke, Identification of sources of Phoenix aerosol by positive matrix factorization, *J. Air Waste Manag. Assoc.*, 2000, **50**, 1308–1320.

77 R. Suarez-Bertoa, A. A. Zardini and C. Astorga, Ammonia exhaust emissions from spark ignition vehicles over the New European Driving Cycle, *Atmos. Environ.*, 2014, **97**, 43–53.

78 H. Zhang, J. Hu, M. Kleeman and Q. Ying, Source apportionment of sulfate and nitrate particulate matter in the Eastern United States and effectiveness of emission control programs, *Sci. Total Environ.*, 2014, **490**, 171–181.

79 P. Pant and R. M. Harrison, Estimation of the contribution of road traffic emissions to particulate matter concentrations from field measurements: A review, *Atmos. Environ.*, 2013, **77**, 78–97.

80 S. M. Gaita, J. Boman, M. J. Gatari, J. B. C. Pettersson and S. Janhäll, Source apportionment and seasonal variation of PM2.5 in a Sub-Saharan African city: Nairobi, Kenya, *Atmos. Chem. Phys.*, 2014, **14**, 9977–9991.

81 A. Thorpe and R. M. Harrison, Sources and properties of non-exhaust particulate matter from road traffic: a review, *Sci. Total Environ.*, 2008, **400**, 270–282.

82 J. K. Gietl, R. Lawrence, A. J. Thorpe and R. M. Harrison, Identification of brake wear particles and derivation of a quantitative tracer for brake dust at a major road, *Atmos. Environ.*, 2010, **44**, 141–146.

83 E. A. Alampay and D. dela Torre, in *Handbook of Climate Change Resilience*, ed. W. Leal Filho, Springer, Cham, Cham, Switzerland, 2020, DOI: **10.1007/978-3-319-93336-8_192**.

84 Y. Zhu, W. C. Hinds, S. Kim and C. Sioutas, Concentration and size distribution of ultrafine particles near a major highway, *J. Air Waste Manag. Assoc.*, 2002, **52**, 1032–1042.

85 K. M. Zhang and A. S. Wexler, Evolution of particle number distribution near roadways—Part I: analysis of aerosol dynamics and its implications for engine emission measurement, *Atmos. Environ.*, 2004, **38**, 6643–6653.

86 X. L. Li, J. S. Wang, X. D. Tu, W. Liu and Z. Huang, Vertical variations of particle number concentration and size distribution in a street canyon in Shanghai, China, *Sci. Total Environ.*, 2007, **378**, 306–316.

87 S.-C. Chen, C.-J. Tsai, C. C. K. Chou, G.-D. Roam, S.-S. Cheng and Y.-N. Wang, Ultrafine particles at three different sampling locations in Taiwan, *Atmos. Environ.*, 2010, **44**, 533–540.

88 J. S. Apte, T. W. Kirchstetter, A. H. Reich, S. J. Deshpande, G. Kaushik, A. Chel, J. D. Marshall and W. W. Nazaroff, Concentrations of fine, ultrafine, and black carbon particles in auto-rickshaws in New Delhi, India, *Atmos. Environ.*, 2011, **45**, 4470–4480.

89 M. Amin, G. Prajati, G. P. Humairoh, R. M. Putri, W. Phairuang, M. Hata and M. Furuuchi, Characterization of size-fractionated carbonaceous particles in the small to nano-size range in Batam city, Indonesia, *Heliyon*, 2023, **9**, e15936.

90 S. Gani, S. Bhandari, K. Patel, S. Seraj, P. Soni, Z. Arub, G. Habib, L. Hildebrandt Ruiz and J. S. Apte, Particle number concentrations and size distribution in a polluted megacity: the Delhi Aerosol Supersite study, *Atmos. Chem. Phys.*, 2020, **20**, 8533–8549.

91 E. Brüggemann, H. Gerwig, T. Gnauk, K. Müller and H. Herrmann, Influence of seasons, air mass origin and day of the week on size-segregated chemical composition of aerosol particles at a kerbside, *Atmos. Environ.*, 2009, **43**, 2456–2463.

92 H. C. Cheung, C. C. K. Chou, M. J. Chen, W. R. Huang, S. H. Huang, C. Y. Tsai and C. S. L. Lee, Seasonal variations of ultra-fine and submicron aerosols in Taipei, Taiwan: implications for particle formation processes in a subtropical urban area, *Atmos. Chem. Phys.*, 2016, **16**, 1317–1330.

93 J. Xue, W. Xue, M. H. Sowlat, C. Sioutas, A. Lolinco, A. Hasson and M. J. Kleeman, Seasonal and Annual Source Appointment of Carbonaceous Ultrafine Particulate Matter (PM(0.1)) in Polluted California Cities, *Environ. Sci. Technol.*, 2019, **53**, 39–49.

94 G.-Y. Lin, G.-R. Lee, S.-F. Lin, Y.-H. Hung, S.-W. Li, G.-J. Wu, H. Ye, W. Huang and C.-J. Tsai, Ultrafine Particles and PM2.5 at Three Urban Air Monitoring Stations in Northern Taiwan from 2011 to 2013, *Aerosol Air Qual. Res.*, 2015, **15**, 2305–2319.

95 P. Pant, A. Shukla, S. D. Kohl, J. C. Chow, J. G. Watson and R. M. Harrison, Characterization of ambient PM2.5 at a pollution hotspot in New Delhi, India and inference of sources, *Atmos. Environ.*, 2015, **109**, 178–189.

96 M. Sillanpää, R. Hillamo, S. Saarikoski, A. Frey, A. Pennanen, U. Makkonen, Z. Spolnik, R. Van Grieken, M. Braniš, B. Brunekreef, M.-C. Chalbot, T. Kuhlbusch, J. Sunyer, V.-M. Kerminen, M. Kulmala and R. O. Salonen, Chemical composition and mass closure of particulate matter at six urban sites in Europe, *Atmos. Environ.*, 2006, **40**, 212–223.

97 Y. Cheng, S. C. Lee, K. F. Ho, J. C. Chow, J. G. Watson, P. K. Louie, J. J. Cao and X. Hai, Chemically-speciated on-road PM(2.5) motor vehicle emission factors in Hong Kong, *Sci. Total Environ.*, 2010, **408**, 1621–1627.

98 J. Gu, Z. Bai, A. Liu, L. Wu, Y. Xie, W. Li, H. Dong and X. Zhang, Characterization of Atmospheric Organic Carbon and Element Carbon of PM2.5 and PM10 at Tianjin, China, *Aerosol Air Qual. Res.*, 2010, **10**, 167–176.

99 G. O. Salako, P. K. Hopke, D. D. Cohen, B. A. Begum, S. K. Biswas, G. G. Pandit, Y.-S. Chung, S. A. Rahman, M. S. Hamzah, P. Davy, A. Markwitz, D. Shagjjamba, S. Lodoysamba, W. Wimolwattanapun and S. Bunprapob, Exploring the Variation between EC and BC in a Variety of Locations, *Aerosol Air Qual. Res.*, 2012, **12**, 1–7.

100 W. Maenhaut, J. Schwarz, J. Cafmeyer and X. Chi, Aerosol chemical mass closure during the EUROTRAC-2 AEROSOL Intercomparison 2000, *Nucl. Instrum. Methods Phys. Res., Sect. B*, 2002, **189**, 233–237.

101 J. C. Chow, D. H. Lowenthal, L. W. Chen, X. Wang and J. G. Watson, Mass reconstruction methods for PM(2.5): a review, *Air Qual., Atmos. Health*, 2015, **8**, 243–263.

102 M. Bae, K. Demerjian and J. Schwab, Seasonal estimation of organic mass to organic carbon in PM2.5 at rural and urban locations in New York state, *Atmos. Environ.*, 2006, **40**, 7467–7479.

103 C. Neusüß, H. Wex, W. Birmili, A. Wiedensohler, C. Koziar, B. Busch, E. Brüggemann, T. Gnauk, M. Ebert and D. S. Covert, Characterization and parameterization of atmospheric particle number-, mass-, and chemical-size distributions in central Europe during LACE 98 and MINT, *J. Geophys. Res.: Atmos.*, 2002, **107**, 8127.

104 C. Neusüß, D. Weise, W. Birmili, H. Wex, A. Wiedensohler and D. S. Covert, Size-segregated chemical, gravimetric and number distribution-derived mass closure of the aerosol in Sagres, Portugal during ACE-2, *Tellus B*, 2000, **52**, 169–184.

105 P. F. DeCarlo, J. G. Slowik, D. R. Worsnop, P. Davidovits and J. L. Jimenez, Particle Morphology and Density Characterization by Combined Mobility and Aerodynamic Diameter Measurements. Part 1: Theory, *Aerosol Sci. Technol.*, 2004, **38**, 1185–1205.

106 W. Phairuang, M. Inerb, M. Hata and M. Furuuchi, Characteristics of trace elements bound to ambient nanoparticles (PM(0.1)) and a health risk assessment in southern Thailand, *J. Hazard. Mater.*, 2022, **425**, 127986.

107 W. Phairuang, T. Chetiyanukornkul, P. Suriyawong, M. Amin, M. Hata, M. Furuuchi, M. Yamazaki, N. Gotoh, H. Furusho, A. Yurtsever, S. Watanabe and L. Sun, Characterizing Chemical, Environmental, and Stimulated Subcellular Physical Characteristics of Size-Fractionated PMs Down to PM(0.1), *Environ. Sci. Technol.*, 2024, **58**, 12368–12378.